Electronic phase transition and amorphization in AuIn$_2$ at high pressure

B. K. Godwal,[1,*] S. Speziale,[1,†] S. M. Clark,[2] J. Yan,[2] and R. Jeanloz[1,3]

[1]*Department of Earth & Planetary Sciences, University of California–Berkeley, California 94720, USA*
[2]*Advanced Light Source, Lawrence Berkeley National Laboratory, 1 Cyclotron Road, Berkeley, California 94720, USA*
[3]*Department of Astronomy, University of California–Berkeley, California 94720, USA*

High-resolution angular-dispersive x-ray diffraction shows that the intermetallic compound AuIn$_2$ retains its initial CaF$_2$ structure to pressures of 23 GPa. We observe continuous broadening of diffraction lines with pressure, leading to amorphization at 24 GPa. The pressure-volume equation of state exhibits an anomaly around 2.7 GPa, in agreement with previous findings and not attributable to nonhydrostaticity. Instead, *ab initio* plane-wave self-consistent field calculations indicate that the observed anomaly is associated with topological changes in the electronic band structure under pressure.

I. INTRODUCTION

Storm *et al.*[1] studied the melting of fluorite- (CaF$_2$) structured AX$_2$ (A=Au, X=In, Ga) compounds to pressures of 5 GPa. Their observation that the fusion curve of AuIn$_2$ has essentially zero slope to about 3 GPa, and then acquires a positive slope with further increase in pressure, suggested the possibility of a pressure-induced transition among crystalline phases. This led to transport and x-ray diffraction studies under pressure, revealing a peak in thermoelectric power (TEP) around 3 GPa and a crystal-structural phase transition beyond 9 GPa.[2,3] As TEP is sensitive to changes in the electronic states at the Fermi level, it was conjectured that the anomaly in the fusion data at 3 GPa could be due to an isostructural electronic (Lifshitz) transition.[4]

Ab initio electronic-structure calculations on AuIn$_2$ suggested that the Fermi level intercepts a band extremum (maximum) at the center (Γ point) of the Brillouin zone under pressure.[2,3] Detailed analysis of the Fermi surface before and after the electronic transition also revealed changes in the Fermi sheet around the Γ point at 5 GPa, and this may be the cause of a nonlinearity in the equation of state.[3,5–8] However, the theoretical estimate of the pressure for these electronic topological transitions (ETTs) was found to be sensitive to the form of the exchange-correlation potential used in the calculations. For example, an ETT occurs at 0.6 GPa using the local-density approximation (LDA) for the exchange-correlation potential,[9–11] as compared with 3.6 GPa obtained from the generalized gradient approximation (GGA).[3,11]

Although the GGA estimate is close to the experimental value, the number of data points is limited and their reliability is uncertain. As the equation-of-state anomaly associated with the ETT is likely to be small, it is important to confirm its presence and magnitude using high-resolution synchrotron-based x-ray diffraction techniques.[3] That is the objective of the present study on the intermetallic compound AuIn$_2$.

II. EXPERIMENT

The sample was prepared by mixing stoichiometric quantities of gold and indium,[1–3] melting the mixture in high vacuum to 900 °C and then cooling to room temperature. It was then ground to a fine powder and examined by x-ray diffraction, which showed that the sample is indeed single-phase cubic structure (Fm3m) AuIn$_2$ having a lattice parameter of a=6.517 Å. After synthesis, the sample material was ground to 5–10 μm average grain size, and loaded into a ~120 μm diameter sample chamber drilled out of a 250-μm thick stainless steel foil that had been indented to a thickness of ~45 μm.

The sample was compressed between two diamond anvils with 230-μm culets, using a mixture of methanol-ethanol-water (16:3:1 volume ratio) as a pressure-transmitting medium. A 10 μm-size fragment of Au foil and a few specks of ruby were loaded as pressure calibrants. High-pressure experiments were performed using a short piston-cylinder diamond-anvil cell (DAC) at beamline 12.2.2 of the Advanced Light Source at Lawrence Berkeley National Laboratory.[12] Powder x-ray diffraction patterns were collected in angle-dispersive geometry. The two sets of measurements used monochromatic radiation, λ =0.48594($\pm$0.00004) and 0.48593 ($\pm$0.00004) Å, and a MAR345 image-plate detector at distances of 295.54 ($\pm$0.01) and 380.1160 ($\pm$0.0012) mm from the sample. The x-ray beam size was approximately 100 μm in the horizontal and vertical directions.

Pressure was determined by the ruby-fluorescence method, using the calibration of Mao *et al.*,[13] and by x-ray diffraction of Au using the 300 K isotherm of Heinz *et al.*[14] and Shim *et al.*[15] The sample-to-detector distance was calibrated by collecting the diffraction pattern of powdered LaB$_6$ at ambient conditions. The software package FIT2D (Ref. [16]) was used both for beam-position and sample-to-detector distance calibrations, and for collapsing the two-dimensional diffraction images to one-dimensional patterns.

As our aim is to document electronic topological transitions manifested through subtle anomalies in the equation of state, we examined the effects of nonhydrostatic stress by collecting data from a sample in which argon was loaded as pressure medium (125 μm diameter sample chamber in a Re gasket indented to a final thickness of 70 μm, and mounted in a symmetric cell having 300 μm-size culets).[17] The symmetric cell has a small angular opening (16°) that limits the number of diffraction lines observed from the sample, but we
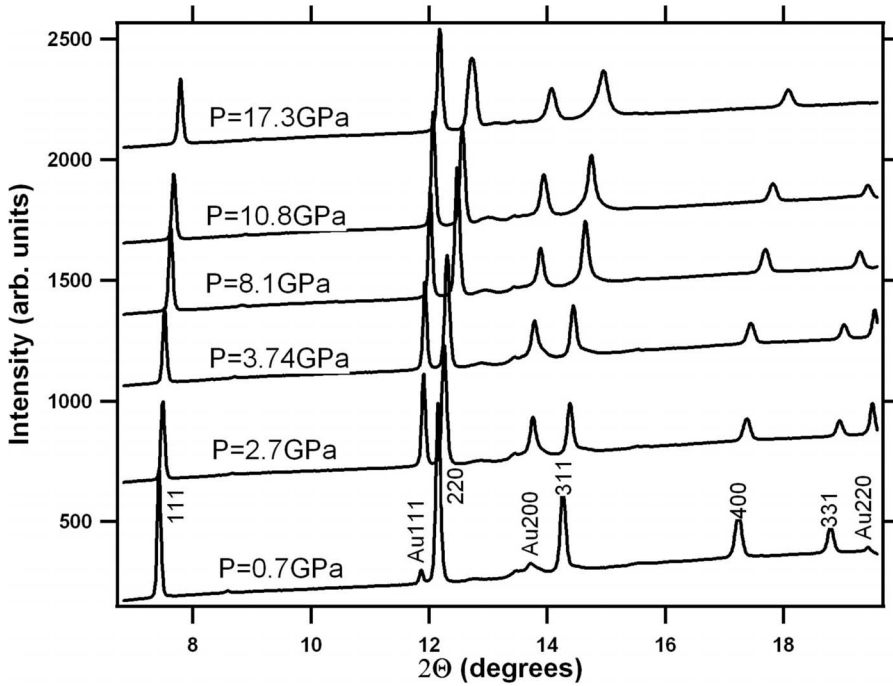
FIG. 1. Evolution of $AuIn_2$ diffraction pattern with pressure.

could still clearly observe the (111), (220), and (311) lines at low pressures; (311) could not be observed clearly above 15 GPa.

III. RESULTS AND DISCUSSION

We found the sample to remain in the initial CaF_2 phase up to 23 GPa (Fig. 1). In order to use the full information of the x-ray diffraction patterns, we have performed full-pattern fits with Le Bail and Rietveld methods by using the two software packages GSAS (Ref. 18) (General Structure Analysis System) and MAUD (Ref. 19) (Material Analysis Using Diffraction) in order to determine the unit-cell parameter and density of $AuIn_2$ at each pressure.

Both the refinements performed with GSAS and with MAUD do not match the observed intensities very well. This is likely due to the effects of continuous line broadening and amorphization, discussed below. However, we were able to use single-peak fits (PeakFIT V4.06) to determine the equation of state because there is generally little overlap among peaks across the diffraction pattern. We also used this approach to obtain the volume of Ar as a function of pressure. The pressure at a given volume was estimated as an average from several measurements across the sample, before and after x-ray diffraction. The pressure uncertainty varied from 4 to 5% between 6 and 20 GPa.

Using the measured zero-pressure volume of V_0 =276.785 ($\pm$0.097) $Å^3$, a third-order Birch-Murnaghan[20,21] fit to the pressure dependence of the $AuIn_2$ unit-cell volume yields a zero-pressure bulk modulus K_{T0}=61.5($\pm$1.0) GPa and pressure derivative $(\partial K_T \partial P)_{T0}$=9.1($\pm$0.3) (Fig. 2); here, subscripts 0 and T indicate zero pressure and isothermal conditions, respectively.

The pressure-volume (P-V) points obtained upon compression and decompression using both argon and methanol-

ethanol-water media are in good agreement with each other, and with the theoretical equation of state discussed in Sec. IV (Fig. 2), showing that quasi-hydrostatic conditions were achieved. In order to better highlight any anomaly in the equation of state of $AuIn_2$, we have plotted the data in terms of Eulerian strain ($f=0.5[(V_0/V)^{2/3}-1]$) and normalized pressure ($F=P/[3f(1+2f)^{5/2}]$) (Fig. 3). This representation effectively shows the slope of the P-V data, such that the intercept and slope at zero strain (f=0) give the bulk modulus (K_{T0}) and its pressure derivative at zero pressure.[14]

The F-f plot shows systematic deviations of the measurements from the single equation of state quoted above, and instead suggests that there are two anomalies in the compression curve, at about 3 GPa (f=0.01–0.0125) and 12 GPa
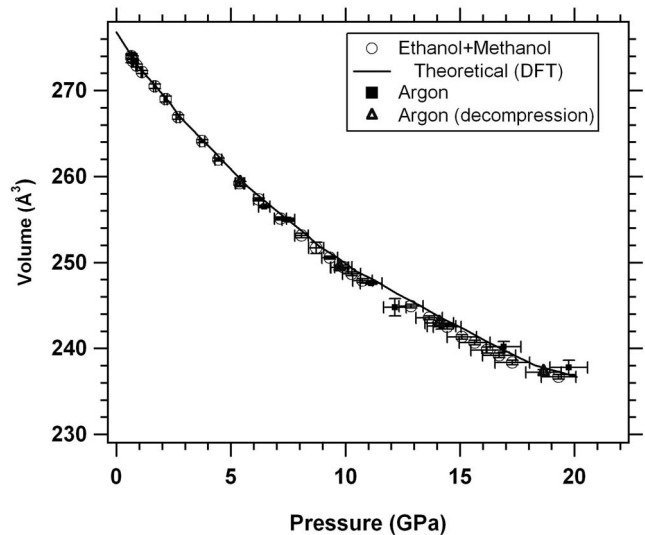

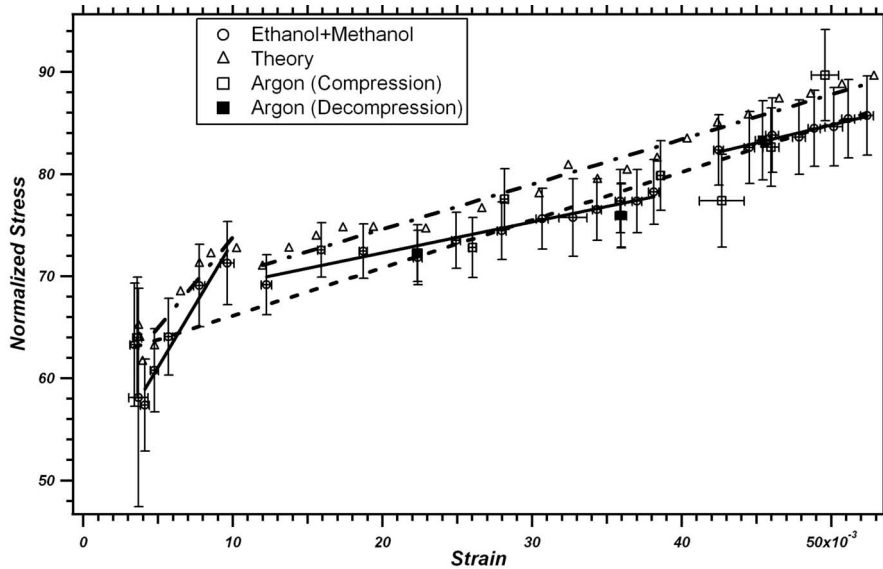FIG. 2. Pressure-volume isothermal equation-of-state measurements for $AuIn_2$ at 300 K.

FIG. 3. Normalized stress F as a function of Eulerian strain f. The solid lines show fits to three regions of the compression curve. The dashed line is a fit of all the data to a single equation of state, and the dashed-dotted line is a fit to two regions of the theoretical results, in agreement with the Vinet fit (see Fig. 4).

($f=0.039-0.042$) (Fig. 3). The two anomalies separate three regions of the compression curve, each characterized by a distinct pressure dependence of the bulk modulus (proportional to the slope of the F-f plot). Fits of the three regions of the F-f curve yield $K_{T0}=56(\pm2)$ GPa and $(\partial K_T/\partial P)_{T0}=18(\pm4)$ for the low-pressure region; $K_{T0}=66.9(\pm3)$ GPa and $(\partial K_T/\partial P)_{T0}=7(\pm0.3)$ for the intermediate region; and $K_{T0}=67.3(\pm2)$ GPa and $(\partial K_T/\partial P)_{T0}=7.5(\pm0.3)$ for the high-pressure region. The low- and intermediate-pressure values of K_{T0} differ substantially, as do the corresponding pressure derivatives, whereas the values for the intermediate- and high-pressure regions are not distinguishable given the uncertainties. In Fig. 3 the dashed line is a fit to the entire data and yields a zero-pressure bulk modulus $K_{T0}=61.5(\pm1.0)$ GPa and pressure derivative $(\partial K_T/\partial P)_{T0}=9.1(\pm0.3)$ consistent with the analysis of the P-V curve above. We note that the data exhibit systematic deviations from this single equation of state.

The results do not depend on the equation-of-state formulation used in analyzing the P-V data, as shown by considering Vinet and colleagues' universal equation of state, i.e., $\ln H$ versus $(1-x)$, where $H=Px^2/[3(1-x)]$ and $x=(V/V_0)^{1/3}$ (Fig. 4).[5–7] There is clearly a discontinuity in slope near 3 GPa, with values of $K_{T0}=56.7(\pm1)$ GPa and $(\partial K_T/\partial P)_{T0}=17.4(\pm4)$ for the low-pressure region and $K_{T0}=64(\pm1)$ GPa and $(\partial K_T/\partial P)_{T0}=8(\pm0.2)$ for the high-pressure region. These agree with the values obtained from the F-f analysis for the low- and intermediate-pressure regions. We thus resolve only one anomaly in the equation of state of $AuIn_2$, at a pressure of 2.7 GPa.

From analysis of the data we noticed continuous broadening of the $AuIn_2$ diffraction lines beyond 11 GPa, with the width of the (220) line doubling between 11 and 20 GPa. The diffraction peaks also decrease in intensity relative to those of gold from 20 GPa onward, vanishing by 24 GPa (Fig. 5). The peak broadening causes the refinement to deteriorate, as
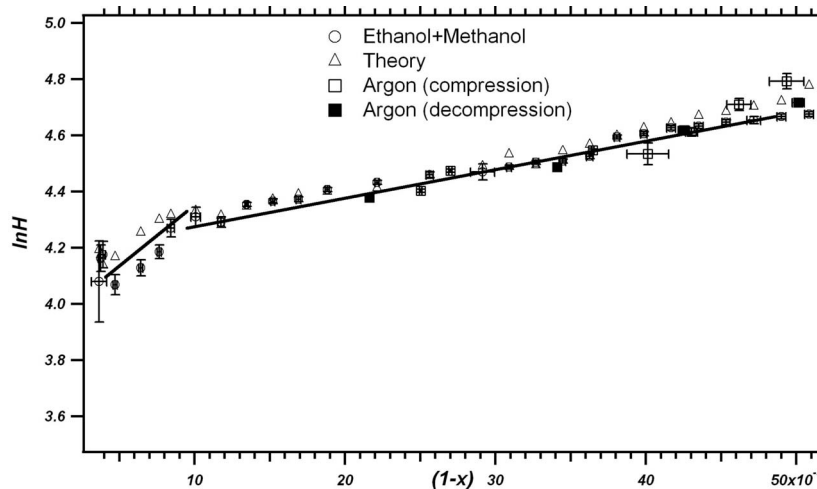

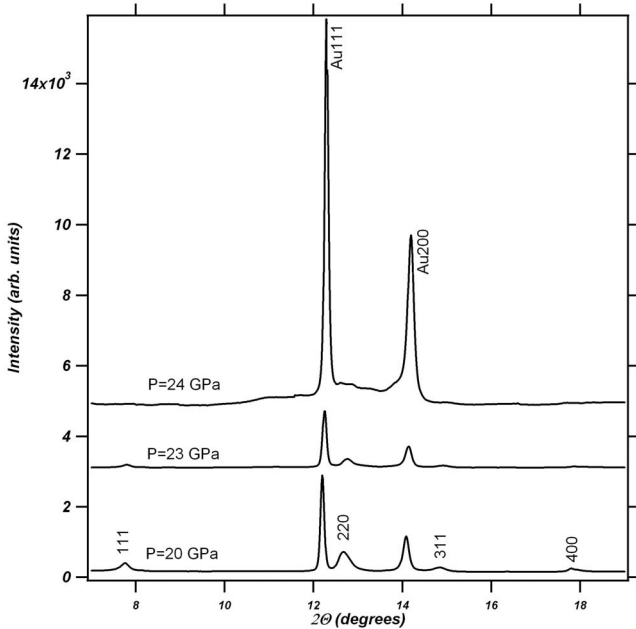FIG. 4. Universal equation of state fit to $AuIn_2$ data.

FIG. 5. Diffraction patterns from 20 GPa onward showing amorphization.

$AuIn_2$ transforms from crystalline to amorphous phases.[22] Upon amorphization of $AuIn_2$, the lattice parameter of Au was found to be 3.9275 ($\pm$0.0012) Å, implying a pressure of 25.5 ($\pm$1.3) GPa from an average of two equations of states;[15,16] for comparison, the average pressure obtained by ruby fluorescence was 24 ($\pm$1.0) GPa, which is in good agreement with the result for gold. We thus put the amorphization pressure at 24 GPa.

On unloading, $AuIn_2$ transforms back to the initial CaF_2 phase. As our measurements with an argon pressure medium are fewer in number and limited to just a few diffraction lines, we are unable to comment about amorphization in those runs. We do not see evidence of a structural transition previously reported[2] around 9 GPa, at least up to 24 GPa. However, the occurrence of amorphization suggests that the CaF_2 phase of $AuIn_2$ is metastable at 20–24 GPa, and it may well be that the crystal-structural transition is sensitive to the degree of nonhydrostaticity present. That shear stresses can affect high-pressure phase transitions in this manner has been documented in systems ranging from Ti (Ref. 23) to $Ca(OH)_2$.[24]

IV. THEORETICAL CALCULATIONS

The difficulty in detecting ETTs under pressure motivates using first-principles theory to assess whether experimentally-observed anomalies may be due to electronic transitions. Total energies have been calculated for $AuIn_2$ using pseudopotential-based plane-wave self-consistent field (PWscf) electronic-structure methods within density-functional theory (DFT).[9,10,25,26] Interactions between ions and valence electrons are described using ultrasoft pseudopotentials, with a 40 Ry plane-wave energy cutoff and a 320 Ry cutoff in the expansion of the augmentation charges. For

Au ($[Xe+4f]5d^{10}6s^1$) and In ($[Kr+4d]4s^25p^1$), the pseudopotential employed the Perdew-Burke-Ernzerhof (PBE) GGA for exchange and correlation effects.[27] This exchange-correlation potential gave results closely matching the experimental compression data.[3] We used a $20\times20\times20$ **k**-point mesh for the Brillouin-zone integration for the fcc structure having 256 k points. Total-energy calculations obtained as a function of volume were used to obtain the zero-K pressure. We added the zero-point vibrational and lattice-thermal contributions to the cold pressure at each volume for comparison with the measured 300 K isotherm, in accordance with the procedure illustrated by Godwal and Jeanloz.[28]

We obtained an equilibrium volume of 279.13 Å^3, in good agreement with the experimental value of 276.79 Å^3. This is in accordance with the fact that GGA potentials typically yield high values for the equilibrium volume. The value of the bulk modulus, its pressure derivative, and the Debye temperature are 64.6 GPa, 8.8 and 162 K, respectively. Though slightly stiffer than the experimental isotherm at high compressions, the computed P-V isotherm is within the error bars of the measured curve (Figs. 2 and 3).

As with the experimental data, the theoretically calculated F-f relation shows two slopes, with $K_{T0}=58$ GPa and $(\partial K_T / \partial P)_{T0}=19$ for the low-pressure region and $K_{T0}=67.2$ GPa and $(\partial K_T / \partial P)_{T0}=8$ for the high-pressure region (Fig. 3). Both the bulk moduli and their pressure derivatives differ substantially between the low- and high-pressure regions, and their values match within error bars those derived from experiment. Good agreement is also found between theory and measurement when comparison is made using the universal equation of state (Fig. 4). The change in F-f and log H slopes is found at 2.8 GPa, which is indistinguishable from the experimental value.

From the detailed electronic band-structure calculations we found the band maximum at the Γ point of the Brillouin zone to be below, but close to, the Fermi level (E_F) at zero pressure. This maximum moves to higher energy with compression, crossing E_F above 3 GPa and resulting in an ETT. Changes in the Fermi sheets due to the electronic transition include a hole appearing around the Γ point above 3 GPa, in agreement with results of previous electronic-structure calculations.[2,3]

V. CONCLUSIONS

$AuIn_2$ remains (meta)stable in the CaF_2 structure to pressures of 23 GPa at 300 K. Diffraction patterns show peak broadening under compression, with amorphization at 24 GPa. Detailed analysis of the compression measurements confirm an anomaly at 2.7–2.8 GPa; as this change in F-f slope (change in curvature of the P-V trend) occurs at low pressure and is reproduced with different pressure media, it cannot be ascribed to freezing of the pressure medium. First-principles calculations support the hypothesis that this anomaly is associated with an ETT: an isostructural transition caused by an extremum in the electronic band structure crossing the Fermi level.

*Present address: Tata Institute of Fundamental Research, Homi Bhabha Road, Colaba, Mumbai-400005, India.

†Present address: GeoForschungsZentrum Potsdam, Division 4.1, Telegrafenberg, 9 24473, Potsdam, Germany.

[1] A. R. Storm, J. H. Wernick, and A. Jayaraman, J. Phys. Chem. Solids **27**, 1227 (1966).

[2] B. K. Godwal, A. Jayaraman, S. Meenakshi, R. S. Rao, S. K. Sikka, and V. Vijayakumar, Phys. Rev. B **57**, 773 (1998).

[3] B. K. Godwal, S. Meenakshi, P. Modak, R. S. Rao, S. K. Sikka, V. Vijayakumar, E. Bussetto, and A. Lausi, Phys. Rev. B **65**, 140101(R) (2002).

[4] I. M. Lifshitz, Zh. Eksp. Teor. Fiz. **38**, 1569 (1960) [Sov. Phys. JETP **11**, 1130 (1960)].

[5] P. Vinet, J. Ferrante, J. H. Rose, and J. R. Smith, J. Geophys. Res. **92**, 9319 (1987).

[6] J. H. Rose, J. R. Smith, F. Guinea, and J. Ferrante, Phys. Rev. B **29**, 2963 (1984).

[7] R. Jeanloz, Geophys. Res. Lett. **8**, 1219 (1981).

[8] S. K. Sikka, Phys. Rev. B **38**, 8463 (1988).

[9] P. Hohenberg and W. Kohn, Phys. Rev. **136**, B864 (1964).

[10] W. Kohn and L. J. Sham, Phys. Rev. **140**, A1133 (1965).

[11] J. P. Perdew and Y. Wang, Phys. Rev. B **45**, 13244 (1992).

[12] M. Kunz, A. A. MacDowell, W. A. Caldwell, D. Cambie, R. S. Celestre, E. E. Domning, R. M. Duarte, A. E. Gleason, J. M. Glossinger, N. Kelez, D. W. Plate, T. Yu, J. M. Zaug, H. A. Padmore, R. Jeanloz, A. P. Alivisatos, and S. M. Clark, J. Synchrotron Radiat. **12**, 650 (2005).

[13] H. K. Mao, J. Xu, and P. M. Bell, J. Geophys. Res. **91**, 4673 (1986).

[14] D. L. Heinz and R. Jeanloz, J. Appl. Phys. **55**, 885 (1984).

[15] S. H. Shim, T. S. Duffy, and K. Takemura, Earth Planet. Sci. Lett. **203**, 729 (2002).

[16] A. P. Hammersley, S. O. Svensson, M. Hanfland, A. N. Fitch, and D. Hausermann, High Press. Res. **14**, 235 (1996).

[17] R. L. Mills, D. H. Liebenberg, D. H. Branson, and L. C. Schmidt, Rev. Sci. Instrum. **51**, 891 (1980).

[18] A. C. Larson and R. B. Von Dreele, Los Alamos National Laboratory Report No. LAUR 86-748, 2004 (unpublished).

[19] L. Lutterotti, S. Matthies, and R. Wenk, IUCR Newsl. **21**, 14 (1999).

[20] F. D. Murnaghan, Proc. Natl. Acad. Sci. U.S.A. **30**, 244 (1944).

[21] F. Birch, Phys. Rev. **71**, 809 (1947).

[22] S. M. Sharma and S. K. Sikka, Prog. Mater. Sci. **40**, 1 (1996).

[23] A. K. Verma, P. Modak, R. S. Rao, B. K. Godwal, and R. Jeanloz, Phys. Rev. B **75**, 014109 (2007).

[24] K. Catalli, S.-H. Shim, and V. B. Prakapenka, Geophys. Res. Lett. **35**, L05312 (2008).

[25] P. Blaha, K. Schwarz, and P. H. Dederichs, Phys. Rev. B **37**, 2792 (1988); P. Blaha, K. Schwarz, and J. Luitz, *Wien 97* (Vienna University of Technology, Vienna, 1997) [improved and updated UNIX version of the original copyrighted WIEN code, which was published by P. Blaha, K. Schwarz, P. Sorantin, and S. B. Trickey, Comput. Phys. Commun. **59**, 399 (1990)].

[26] For PWscf see http://www.pwscf.org

[27] J. P. Perdew, K. Burke, and M. Ernzerhof, Phys. Rev. Lett. **77**, 3865 (1996).

[28] B. K. Godwal and R. Jeanloz, Phys. Rev. B **41**, 7440 (1990); The combined pressure from zero-point and lattice vibrations at ambient conditions was less than 1 GPa.